First-Order Mass Transfer in a Vortex-Dispersion Zone of an Axisymmetric Groove: Laboratory and Numerical Experiments

Kim, Young-Woo† Kang, Kijun*

Abstract

Solute transport through a groove is affected by its vortices. Our laboratory and numerical experiments of dye transport through a single axisymmetric groove reveal evidence of enhanced spreading and mixing by the vortex, i.e., a new kind of dispersion called here the vortex dispersion. The uptake and release of contaminants by vortices in porous media is affected by the flow Reynolds number. The larger the flow Reynolds number, the larger is the vortex dispersion, and the larger is the mass-transfer rate between the mobile zone and the vortex. The long known dependence of the mass-transfer rate between the mobile and "immobile" zones in porous media on flow velocity can be explained by the presence of vortices in the "immobile" zone and their uptake and release of contaminants.

Keywords *: solute transport, mass tranfer, vortex, dispersion, numerical analysis, computational fluids dynamics*

1. Introduction

The roles of advection-dominated (mobile) and diffusion-dominated (immobile) zones in contaminant transport in porous media have been recognized since the mobile-immobile zone (MIM) model was introduced by Coats and Smith (1964) in petroleum engineering and by van Genuchten and Wierenga (1976) in hydrology and soil-science. This model produces breakthrough curves (BTCs) with exponential tails. Further refined by accounting for multiple mass transfer rates (Villeramaux, 1981, 1987, 1990; Brusseau *et al.*, 1989; Valocchi, 1990; Sardin *et al.*, 1991; Haggerty and Gorelick, 1995; Haggerty *et al.*, 2000; Meigs and Beauheim, 2001) or even fractal mass transfer rates (Schumer *et al.*, 2003), the MIM model has been used to interpret numerous column experiments and field tracer tests, and has led to a vast body of technical literature. The multirate MIM model can describe even seemingly anomalous BTCs with power-law tails rather than exponential tails (Werth *et al.*, 1997; Cunnigham *et al.*, 1997; Haggerty and Gorelick, 1998; Haggerty *et al.*, 2001; Meigs and Beauheim, 2001). Haggerty and Gorelick (1995) pointed out that the mobile/immobile zone and multirate mass transfer equations available in the literature are closely related to the basic mass transfer equation:

$$\frac{\partial C_{im}}{\partial t} = \alpha (C_m - C_{im}) \tag{1}$$

where C_{im}, C_m, t, and α are concentration in the immobile zone, concentration in the mobile zone, time, and a first-order rate coefficient, respectively. This equation can be easily solved subject to

$$C_m(t) = C_m = const \tag{2}$$

and

† 책임저자, 정회원 · 호서대학교 자동차공학과 전임강사
Tel: 041-540-5810 ; Fax: 041-540-5818
E-mail: ywkim@hoseo.edu
* 호서대학교 자동차공학과 교수

• 이 논문에 대한 토론을 2011년 2월 28일까지 본 학회에 보내주시면 2011년 4월호에 그 결과를 게재하겠습니다.

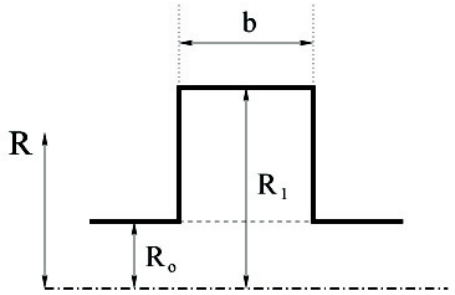

Fig. 1 Schematic of an axisymmetric groove

$$C_{im}(0) = C_0 \tag{3}$$

is given by an exponential decay

$$\frac{C_{im}(t) - C_m}{C_0} = \exp(-\alpha t) \tag{4}$$

Kim *et al.* (2010) considered an axisymmetric groove presented in Fig. 1 with a mobile zone in the domain $0 \le R \le R_0$ and an immobile zone in the domain $R_0 \le R \le R_1$. As they did, we drop the subscript in the immobile-zone concentration and denote it from now on by C. With molecular diffusion D, we also define the dimensionless time

$$\tau = \frac{D\,t}{(R_1 - R_0)^2} \tag{5}$$

and the dimensionless concentration

$$c = \frac{C - C_m}{C_0} \tag{6}$$

With Eq. (6)~Eq. (5) we can non-dimensionalize the MIM model, Eq. (4), as

$$c(\tau) = \exp\left[-\frac{\alpha (R_1 - R_0)^2}{D}\,\tau\right] = \exp(-S t) \tag{7}$$

Assuming completely still immobile zone in the groove, Kim *et al.* (2010) derived an exact analytic model of mass transfer into or from this zone. The solution is in the form of a series of exponentials. However, for sufficiently long dimensionless times, $\tau \ge \tau_0 \approx 0.15$, the first term in the series dominates, and the solution is expressed by a single exponential

$$\bar{c}(\tau) = c_0 \exp[-S(y)\,\tau] \tag{8}$$

where c_0 is a dimensionless apparent initial concentration (Kim *et al.*, 2010), while

$$S(y) = \frac{12(1-y)^2\,(3 - 4y^2 + y^4 + 4\ln y)}{(y^2-1)(17 - 13y^2 + 2y^4) + 12\ln y\,(-3 + 2y^2 + 2\ln y)} \tag{9}$$

is the dimensionless groove shape factor that depends on groove geometry parameter

$$y = R_0 / R_1 \tag{10}$$

A comparison of Eq. (8) and Eq. (7) yields the mass transfer coefficient of the MIM model

$$\alpha = \frac{S(y)\,D}{(R_1 - R_0)^2} \tag{11}$$

Derived for a completely still immobile zone in the groove, this mass-transfer coefficient for the MIM model is independent of the mobile-zone flow velocity. This, however, is well known to be contrary to the number of laboratory and field observations (Brusseau, 1992; Bajracharya and Barry, 1997; and others). This is not surprising, as it has been long pointed out (Gluecakauf, 1955; Rao *et al.*, 1980ab; Haggerty *et al.*, 2004; Kim *et al*, 2010; and others) that the mobile-immobile zone models do not fully represent the physics of mass transfer.

We note that it is already well known that vortices can form in grooves with smooth edges (Hemmat and Borhan, 1995; Kitanidis and Dykaar, 1997) and, particularly, in grooves with sharp edges (Cao and Kitanidis, 1998; Cieslicki and Lasowska, 1999). However, a special role that these vortices may play in mass transfer has not yet been appreciated. In fact, Kitanidis and Dykaar (1997) note in discussing the vortices that arose in their 2-D sinusoidal groove, that they form "what is practically an immobile zone."

The purpose of this paper is i) to study in laboratory and numerical experiments the mass transfer between a vortex zone and a mobile zone of a groove, ii) to demonstrate that the current classi-fication of groove water into mobile and immobile zones is not sufficient, and iii) to demonstrate that the so far unaccounted for vortex zone plays an important role in contaminant transport through porous media.

2. Methodology for Laboratory and Numerical Experiments

Fig. 2 presents the diagrams of laboratory setup. With $2R_0$= 0.25inches and $2R_1$=3.5inches, $y = R_0/R_1$=14. It then follows from Eq. (9), that the groove-shape factor is fixed at $S(14) \approx 5.265$. We used a quasi-conservative tracer Fluorescein in our entire laboratory experiments. First, a 100 ppb solution of Fluorescein was introduced up to the 50-inch mark on the vertical pipe, measured from the outlet. It filled our axisymmetric groove and a part of the pipe leading to it. Next, the rest of the pipe and the reservoir were filled up with distilled water from the top. Then the automatic collection of the concentration data was started simultaneous- ly with opening the valve. Fluorescein concentration was measured with Turner Designs Model 10-AU Field Fluorometer capable of detecting concent-rations of Fluorscein to parts per trillion. Each data set was collected three times to confirm and ensure repeatability of the experiments.

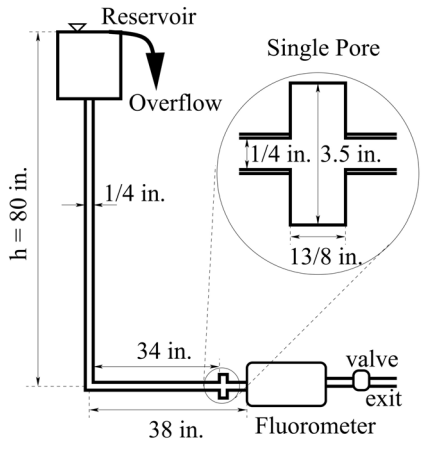

Fig. 2 Schematic of laboratory setup

Developed and maintained by Fluent Inc. in Lebanon, New Hampshire, the commercially available computational fluid dynamics (CFD) software FLUENT has been successfully employed in numerous CFD studies in chemical and mechanical engineering, atmospheric and aerosol sciences, and others (Chan *et al.*, 2002; Sanyal *et al.*, 1999; He and Ahmadi, 1998; Ranade and Dometi, 1996). FLUENT is also suitable for our purpose. We use it assuming Fickian molecular diffusion of Fluorescein with molecular diffusion of $D=0.5\times10^{-9}\mathrm{m}^2/\mathrm{s}$ (de Beer *et al.*, 1997).

For convergence test, we generated a single groove model with 5 different meshes. The two densest meshes, with 63,000 and 80,000 nodes, produced practically identical results. Consequently, we used the 63,000-node mesh in all our simulations reported here.

Our numerical and laboratory experimental flows through the axisymmetric groove, described in Figs. 1 and 2, are characterized by the Reynolds number defined as

$$Re = \frac{\bar{v}\,(2R_0)}{\nu} = \frac{Q(2R_0)}{\pi R_0^2\,\nu} = \frac{2Q}{\pi R_0\,\nu} \qquad (12)$$

where $\bar{v}$ is the mean velocity, R_0 is the groove entrance radius defined in Fig. 1, ν is the kinematic viscosity of water, and Q is its volumetric flowrate.

3. Results from Laboratory Experiments

In Fig. 3 we demonstrate that the lab experiments pass the repeatability test, i.e., the breakthrough curves (BTCs) from three consecutive experiments attempted in the same conditions (same Re, same C_0) are very close to each other. The initial segments of the BTCs are complex as they reflect the combined effect of Fluorescein being diffused from the groove into the main channel, being flushed by the flow there, and being delayed by Taylor dispersion. In their later segments, the BTCs seem to set into the expected exponential decay. Some of them are serrated,

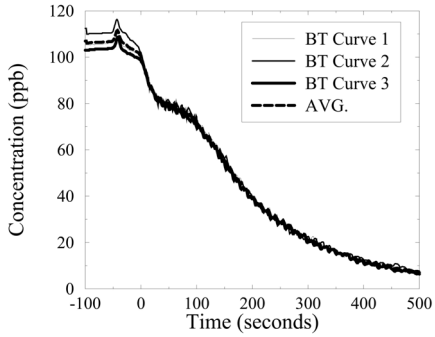

(a) Re ≈ 176

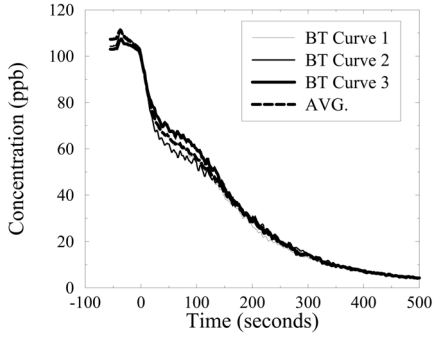

(b) Re ≈ 236

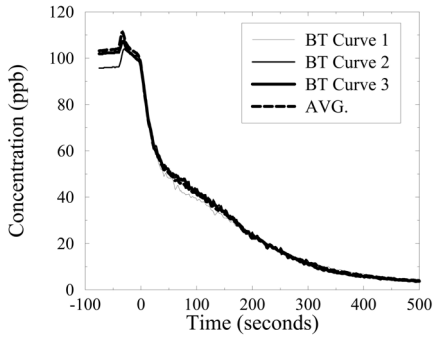

(c) Re ≈ 283

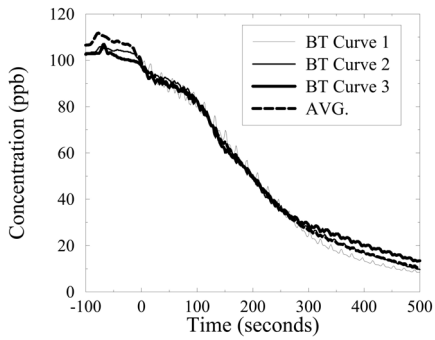

(d) Re ≈ 316

Fig. 3 The results of the repeatability test for the axisymmetric-groove experiments

as the raw concentration measurements by the fluorometer oscillate around the true values. Although the average concentrations are not as much serrated, we

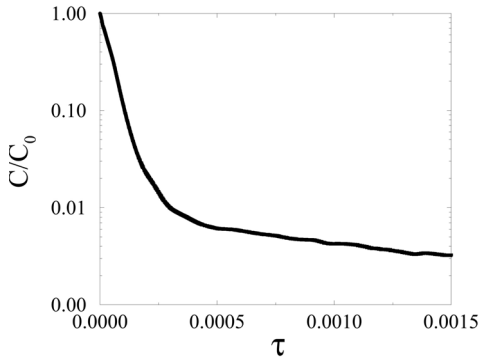

(a) Re = 283

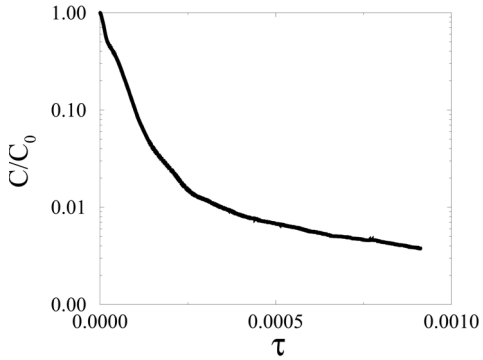

(b) Re = 316

Fig. 4 Log-linear plot of dimensionless concentration and time

further smoothed them with an averaging window of 5 data points.

In Fig. 4 we re-plot these smoothed average BTCs in log-linear coordinates, but this time versus dimensionless time. What is striking about this figure is how quickly the exponential decay sets in: roughly for $\tau > 0.0005$ rather than for $\tau > \tau_0 = 0.15$ derived by Kim *et al.* (2010) for the MIM model with perfectly still immobile zone. The exponential decay in concentration of the dye released by the vortex sets thus in about 300 times faster than it does from the perfectly still (no vortex) immobile zone. This is a clear experimental evidence of the additional solute spreading and mixing by the vortex, i.e., a new kind of (so far unaccounted for) dispersion at work. We call it the vortex dispersion.

4. Results from Numerical Analysis

In Fig. 5 we present the numerically calculated

streamlines. It is evident that for $Re<1$, the streamlines stay approximately constant and are very close to those for the creeping (Stokes) flow. The vortex is then symmetrical and is pushed into the groove cavity. For $1<Re<100$ the morphology of the vortex varies significantly with Re.

For $Re>100$ the vortex occupies the whole groove space with the exception of the rapid-flow channel of $0<R<R_0$ and its morphology doesn't change much. For different Reynolds numbers, Fig. 6 presents the dimensionless concentrations, calculated from our numerical experiments, versus dimensionless time. This figure tells us again not only what we learned from Fig. 4, i.e., how quickly the exponential decay of concentration sets in, but also that the answer is affected by the vortex dispersion. Fig. 6, clearly demonstrates that in log-linear coordinates the linear segment of a simulated BTC has the slope that depends on the Reynolds number. The magnitude of this slope yields the corresponding effective mass-transfer coefficient, α_{eff}, which turns out to be much larger than the mass-transfer coefficient α predicted by the MIM model, Eq. (11), for a perfectly still (no-vortex) immobile zone.

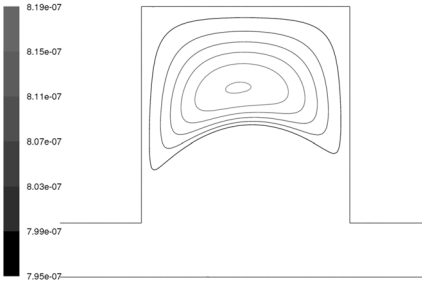

(a) Re = 1

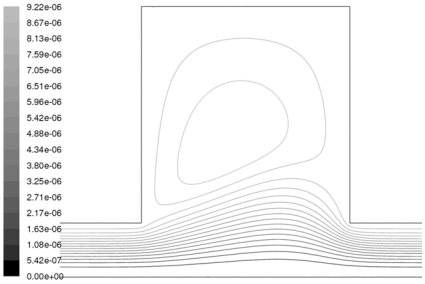

(b) Re = 10

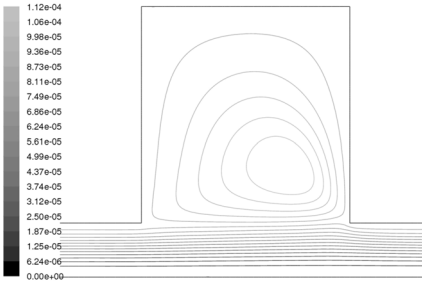

(c) Re = 100

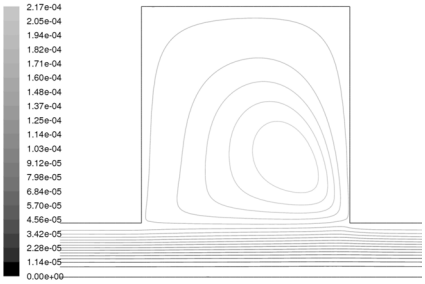

(d) Re = 200

Fig. 5 Streamline Contour Plots

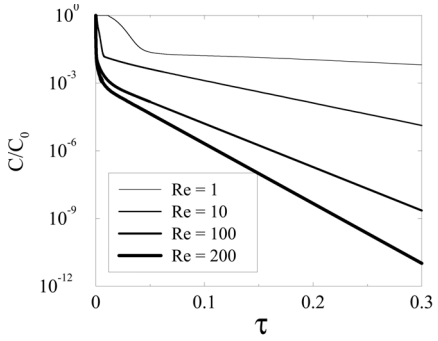

(a)

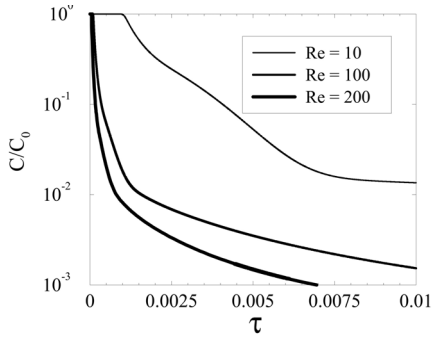

(b)

Fig. 6 Dimensionless Concentration, C/C_0, vs Dimentionless Time, τ, for (a) long times (b) short times

In Fig. 7 we present the relationship between α_{eff}/α, calculated from the slopes of our BTCs presented in Fig. 6, to the Reynolds number (or mean groove-scale velocity). We also note that the effective mass-transfer coefficient $\alpha_{eff}(Re)$ can be interpreted via Eq. (11) with molecular diffusion, D replaced by vortex dispersion $D_{eff}(Re)$. We note that

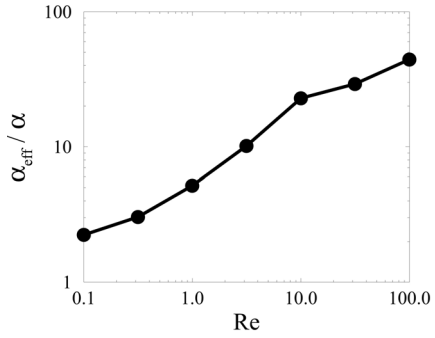

Fig. 7 Dimensionless effective mass-transfer coefficient α_{eff}/α vs Re

$$\frac{D_{eff}(Re)}{D} = \frac{\alpha_{eff}(Re)}{\alpha} \tag{13}$$

Fig. 7 represents another clear evidence of the additional solute spreading and mixing provided by the vortex, i.e., a new kind of dispersion: the vortex dispersion. To our knowledge, this is the first explanation of the origin of the velocity dependence of the mass-transfer coefficient observed and reported by Brusseau (1992), Bajracharya and Barry (1997), and others.

5. Conclusions

Our laboratory and numerical experiments of Fluorescein transport through a single axisymmetric groove reveal clear evidence of additional solute spreading and mixing by the vortex, i.e., a kind of dispersion: the vortex dispersion. The uptake and release of contaminants by vortices in porous media is affected by the flow Reynolds number. The larger the flow Reynolds number, the larger is the vortex dispersion, and the larger is the mass-transfer rate between the mobile zone and the vortex.

The long known dependence of the mass-transfer rate between the mobile and "immobile" zones in porous media on flow velocity, observed and reported by Brusseau (1992), Bajracharya and Barry (1997), and others, can be explained by the presence of vortices in the "immobile" zone and their uptake and release of contaminants.

References

Bajracharya, K., Barry, D.A. (1997) Nonequilibrium Solute Transport Parameters and Their Physical Significance: Numerical and experimental results, *J. Contam. Hydrol.*, 24(3-4), pp.185~204.

Brusseau, M.L., Jessup, R.E., Rao, P.S.C. (1989) Modeling the Transport of Solutes Influenced by Multiprocess Nonequilibrium, *Water Resour. Res.*, 25(9), pp.1971~1988.

Brusseau, M.L. (1992) Nonequilibrium Transport of Organic Chemicals-The Impact of Pore-Water Velocity, *J. Contam. Hydrol.*, 9(4), pp.353~368.

Cao, J., Kitanidis, P.K. (1998) Adaptive Finite Element Simulation of Stokes flow in Porous Media, *Adv. Water Res.*, 22(1), pp.17~31.

Cieslicki, K., Lasowska, A. (1999) Experimental Investigations of Steady flow in a Tube with Circumferential Wall Cavity, *Journal of Fluids Engineering*, 121, pp.405~409.

Coats, K.H., Smith, B.D. (1964) Dead-End Pore Volume and Dispersion in Porous Media, *Soc. Petrol. Eng. J.*, 4, pp.73~84.

Cunningham, J.A., Werth, C.J., Reinhard, M., Roberts, P.V. (1997) Effects of Grain-Scale Mass Transfer on the Transport of Volatile Organics Through Sediments.1. Model development, *Water Resour. Res.*, 33(12) pp.2713~2726.

de Beer, D., Stoodley, P., Lewandowski, Z. (1997) Measurement of Local Diffusion Coefficients in Biofilms by Microinjection and Confocal Microscopy, *Biotechnol. Bioeng.*, 53(2), pp.151~158.

Glueckauf, E. (1955) Theory of Chromatography, part 10, Formulae for Diffusion into Spheres and their Application to Chromatography, *Trans. Faraday Soc.*, 51, pp.1540~1551,

Haggerty, R., Gorelick, S.M. (1995) Multiple-Rate Mass-Transfer for Modeling Diffusion and Surface-Reactions in Media with Pore-Scale Heterogeneity, *Water Resour. Res.*, 31(10), pp. 2383~2400.

Haggerty, R., Gorelick, S.M. (1998) Modeling Mass Transfer Processes in Soil Columns with Pore-Scale Heterogeneity, *Soil Sci. Soc. Am. J.*, 62(1), pp.62~74.

Haggerty, R., McKenna, S.A., Meigs, L.C. (2000) On the Late-Time Behavior of Tracer Test Breakthrough Curves, *Water Resour. Res.*, 36(12),

pp.3467~3479.

Haggerty, R., Fleming, S.W., Meigs, L.C., McKenna, M.C. (2001) Tracer Tests in a Fractured Dolomite. 2. Analysis of Mass Transfer in Single-well Injection-Withdrawal Tests, *Water Resour. Res.*, 37(5), pp.1129~1142,

Haggerty, R., Harvey, C.F., von Schwerin, C.F., Meigs, L.C. (2004) What Controls the Apparent Timescale of Solute Mass Transfer in Aquifers and Soils, A Comparison of Experimental Results, *Water Resour. Res.*, 40(1): Art. No. W01510.

He, C.H., Ahmadi, G. (1998) Particle Deposition with Thermophoresis in Laminar and Turbulent Duct Flows, *Aerosol Sci. Tech.*, 29(6), pp.525~546.

Hemmat, M., Borhan, A. (1995) Creeping Flow Through Sinusoidally Constricted Capillaries, *Phys. Fluids*, 7(9), pp.2111~2121

Kim Y.W, Seo, B.M., Hwang, S.M., Park, C.S. (2010) Derivation of the First-Order Mass-Transfer Equation for a Diffusion-Dominated Zone of a 2-D Pore, *KSME-B*, 34(2), pp.99~103

Kitanidis, P.K., Dykaar, B. (1997) Stokes Flow in a Slowly Varying Two-Dimensional Periodic Pore, *Trans. Porous Media*, 26, pp.89~98.

Leneweit, G., Auerbach, D. (1999) Detachment Phenomena in Low Reynolds Number Flows Through Sinusoidally Constricted Tubes, *J. Fluid Mech.*, 387, pp.129~150.

Meigs, L.C., Beauheim, R.L. (2001) Tracer Tests in a Fractured Dolomite. 1. Experimental Design and Observed Tracer Recoveries, *Water Resour. Res.*, 37(5), pp.1113~1128.

Ranade, V.V., Dommeti, S.M.S. (1996) Computational Snapshot of Flow Generated by Axial Impeller in Baffled Stirred Vessels, *Chem. Eng. Res. Design*, 74(A4), pp.476~484.

Rao, P.S.C., Rolston, D.E., Jessup, R.E., Davidson, J.M. (1980) Solute Transport in Aggregated Porous Media-Theoretical and Experimental Evaluation, *Soil Sci. Soc. Am. J.*, 44(6), pp.1139~1146.

Rao, P.S.C., Jessup, R.E., Rolston, D.E., Davidson, J.M., Kilcrease, D.P. (1980) Experimental and Mathematical Description of Non-Adsorbed Solute Transfer by Diffusion in Spherical Aggregates, *Soil Sci. Soc. Am. J.*, 44(4), pp.684~688.

Sanyal, J., Vasquez, S., Roy, S., Dudukovic, M.P. (1999) Numerical Simulation of Gas-Liquid Dynamics in Cylindrical Bubble Column Reactors, *Chem. Eng. Sci.*, 54(21), pp.5071~5083.

Sardin, M., Schweich, D., Leij, F.J., van Genuchten, M.T. (1991) Modeling the Nonequilibrium Transport of Linearly Interacting Solutes in Porous Media-A Review, *Water Resour. Res.*, 27(9), pp.2287~2307.

Schumer, R., Benson, D.A., Meerschaert, M.M., Baeumer, B. (2003) Fractal Mobile/Immobile Solute Transport, *Water Resour. Res.*, 39(10), Art. No. 1296.

Stehfest, H. (1970) Numerical Inversion of Laplace Transforms, *Commun.ACM.* 13, pp.47~49.

Valocchi, A.J. (1990) Use of Temporal Moment Analysis to Study Reactive Solute Transport in Aggregated Porous Media, *Geoderma*, 46(1-3), pp.233~247.

van Genuchten, M.T., Wierenga, P.J. (1976) Mass Transfer Studies in Sorbing Porous Media. 1. Analytical Solutions, *Soil Sci. Soc Am. J.*, 40, pp.473~480.

Villeramaux, J. (1981) Theory of Linear Chromatography, in *Percolation Processes, Theory and Applications*, edited by A.E. Rodrigues and D. Tondeur, *NATO ASI Ser., Ser. E,* 33, pp.83~140.

Villeramaux, J. (1987) Chemical Engineering Approach to Dynamic Modeling of Linear Chroma-Tography: A Flexible Method for Representing Complex Phenomena from Simple Concepts, *J. Chromatogr.* 406, pp.11~26,

Villeramaux, J. (1990) Dynamics of Linear Interactions in Heterogeneous Media: A Systems Approach, *J. Pet. Sci. Eng.*, 4(1), pp.21~30.

Werth, C.J., Cunningham, J.A., Roberts, P.V., Reinhard, M. (1997) Effects of Grain-Scale Mass Transfer on the Transport of Volatile Organics Through Sediments. 2. Column Results, *Water Resour. Res.*, 33(12), pp.2727~2740

● 논문접수일 2010년 10월 30일
● 논문심사일 2010년 11월 4일
● 게재확정일 2010년 11월 29일